Dadgar et al., http://www.jcb.org/cgi/content/full/jcb.201402079/DC1

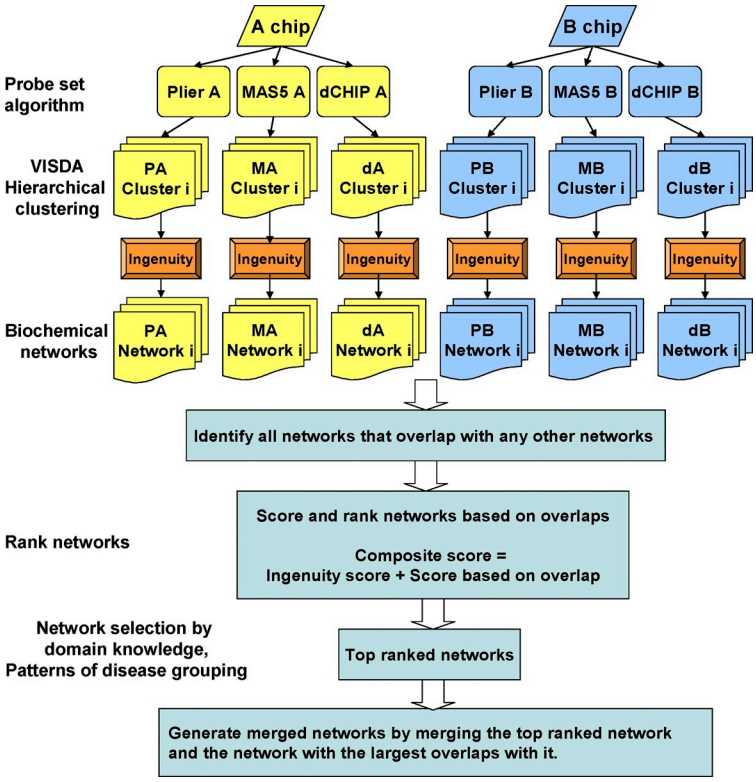

Figure S1. **Flow chart of the data integration and biochemical network analysis on the 12-group human muscle transcriptional profiling data.**

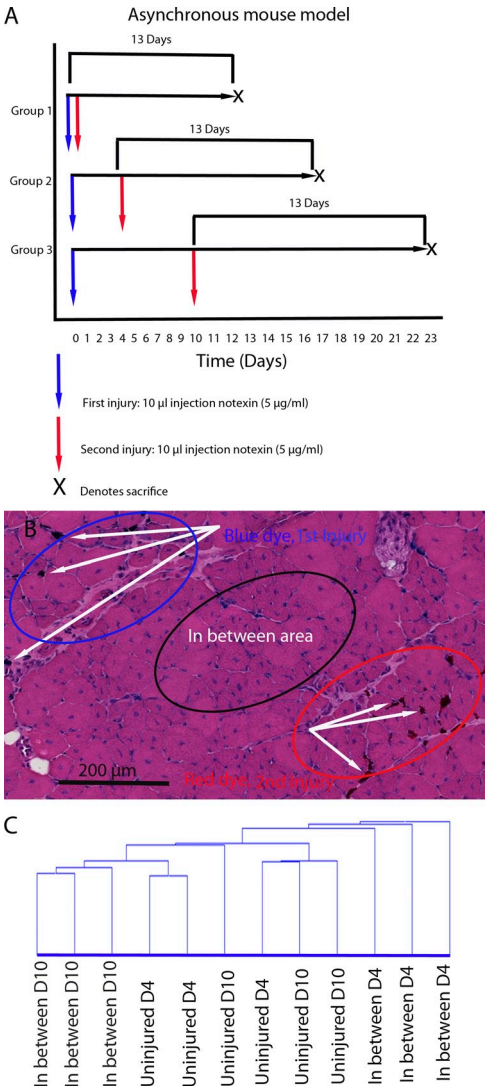

Figure S2. **LCM methods and chip clustering of mRNA profiles of LCM regions of multiply injured muscle.** (A) A schematic of the experimental design of the asynchronous remodeling system used. Figure shows the time line of injections and sacrifice of mice. 0-, 4-, and 10-d designs are shown; however, additional time points (1, 2, and 5 d) were also performed (see Establishing a model of asynchronous muscle regeneration). (B) Shown is a hematoxylin and eosin–stained muscle tissue, showing the general features of each muscle studied with the asynchronous remodeling experimental system. Two intramuscular injections of notexin were performed, the first labeled with blue tattoo dye and the second labeled with red tattoo dye. Arrows show the red and blue tattoo dyes marking the two injury sites. Both areas show the colored dye as well as the preponderance of myofibers with centralized nuclei indicative of degeneration and regeneration. LCM methods were used to isolate each injection site as well as the region of muscle in between the two injection sites. (C) Shown is an unsupervised hierarchical clustering dendrogram of Illumina mRNA microarray data of entire microarrays (chip-based clustering). This reveals the overall relationship of the different arrays and provides an indication of signal/noise balance in the microarray study. This shows excellent clustering of replicates (arrays from different cryosections of muscle), suggesting a good signal/noise balance.

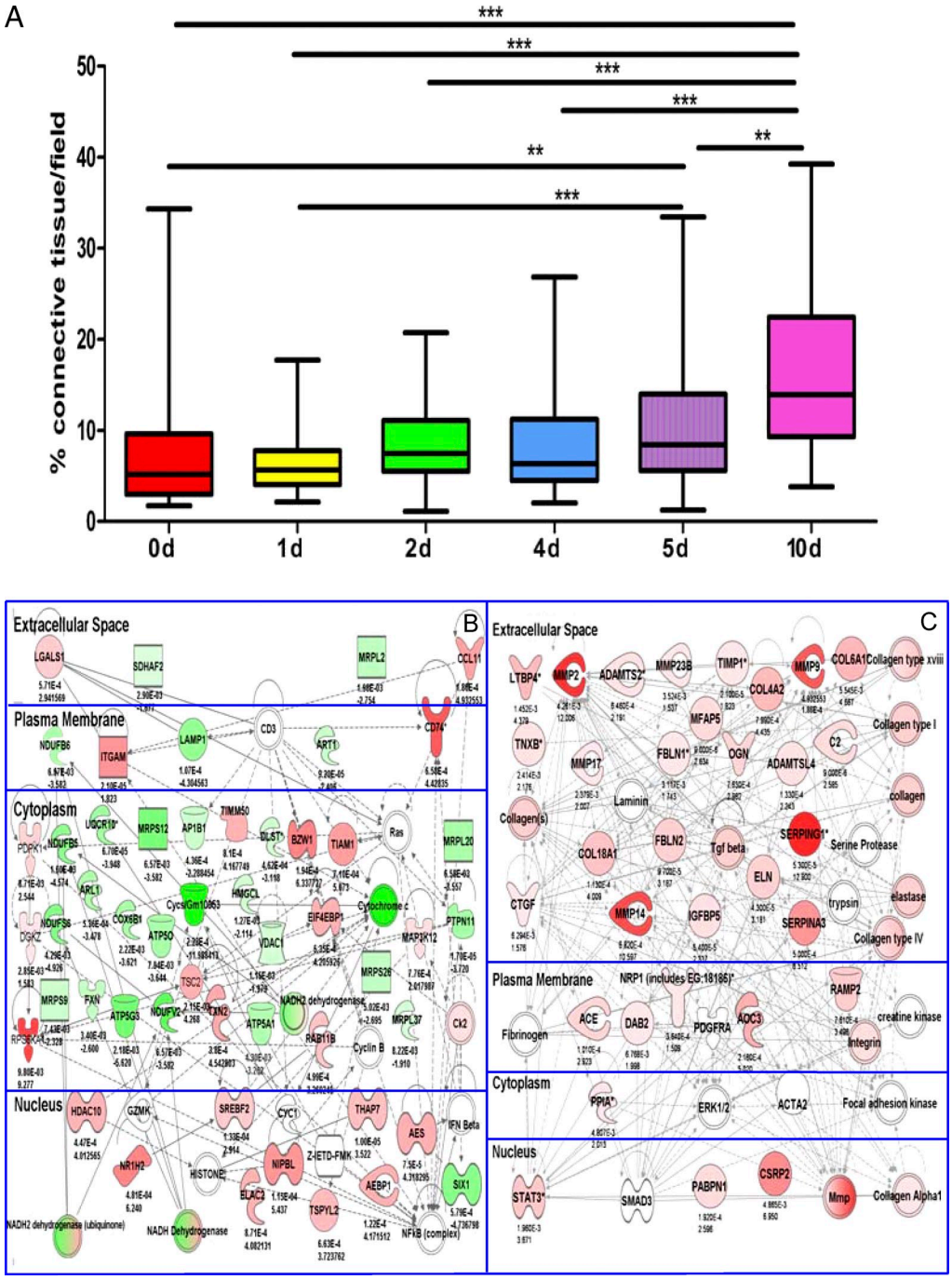

Figure S3. **Quantitative analysis of endomysial fibrosis in asynchronous remodeled muscle samples.** (A) Shown are box and whisker plots for quantitation of the percentage of Van Gieson–positive material (fibrosis; y axis) from asynchronously remodeling muscles with injections spaced at the indicated time points (0, 1, 2, 4, 5, and 10 d apart). There is a significantly greater amount of interstitial connective tissue in muscles in the 10-d reinjury group compared with all other reinjury time spacings (horizontal bars show p-values between specific groups). Images of Van Gieson–stained reinjured muscle sections were analyzed in ImageJ to determine the amount of interstitial connective tissue per field of tissue (n = 4 muscles per group; *, $P < 0.05$; **, $P < 0.01$; ***, $P < 0.001$; all data were analyzed by Kruskal–Wallis and Dunn's multiple comparison test). (B and C) mRNA profiles of the region of muscle tissue in between injection sites shows different patterns for injections spaced 4 d apart versus 10 d apart**.** Shown are the top-ranked IPA networks from mRNA expression profiles. These are the same network images shown in Fig. 4 and Fig. 5 but are aligned adjacent each other, with cross-network indication of subcellular localization of encoded proteins (red dashed lines). This shows that cytoplasmic and nuclear proteins are predominant in 4-d mRNA profiles (mitochondrial and inflammatory proteins), whereas extracellular matrix proteins predominate in the 10-d mRNA profiles. Numbers indicate p-value (top) and fold change (bottom).

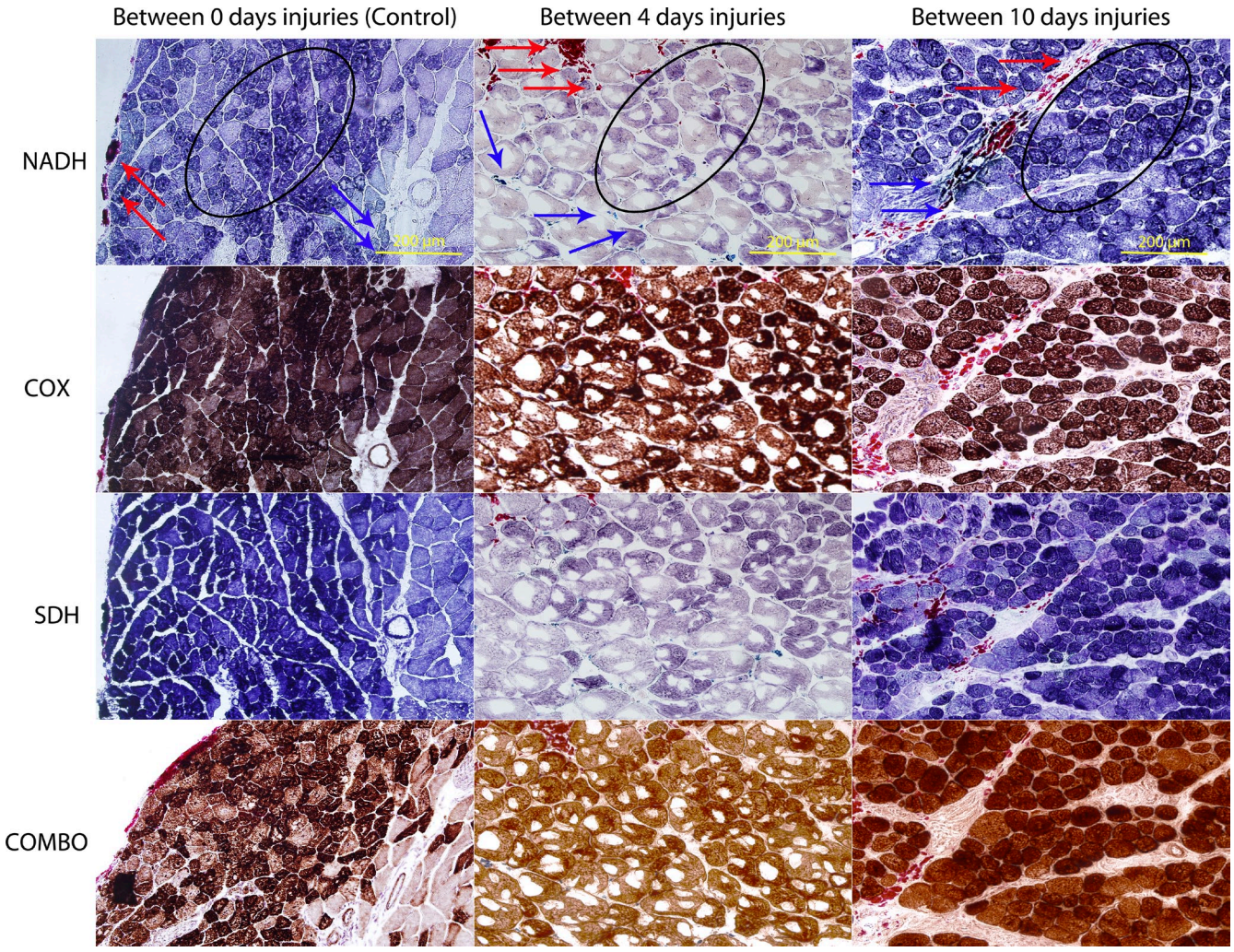

Figure S4. **Histochemical stains for mitochondrial activity show a relative loss of mitochondrial oxidative phosphorylation in the area between injuries spaced 4 d apart.** Shown are the indicated muscles (n = 3 per group) stained for the activity of mitochondrial enzymes NADH, COX, SDH, and a combination (COX and SDH). Blue and red arrows indicate the first and second injury sites, respectively. Ovals show laser capture microdissected areas. Control (0-d spaced regions with synchronous regeneration after injury) and in-between injections spaced 10 d apart show strong staining with all three mitochondrial activities, indicating recovery of oxidative phosphorylation. The regenerated region between the injury sites staged 4 d apart shows poor differentiation of fiber types, with relative loss of oxidative phosphorylation capacity. These data validate the mRNA profiling data shown in Fig. 4.

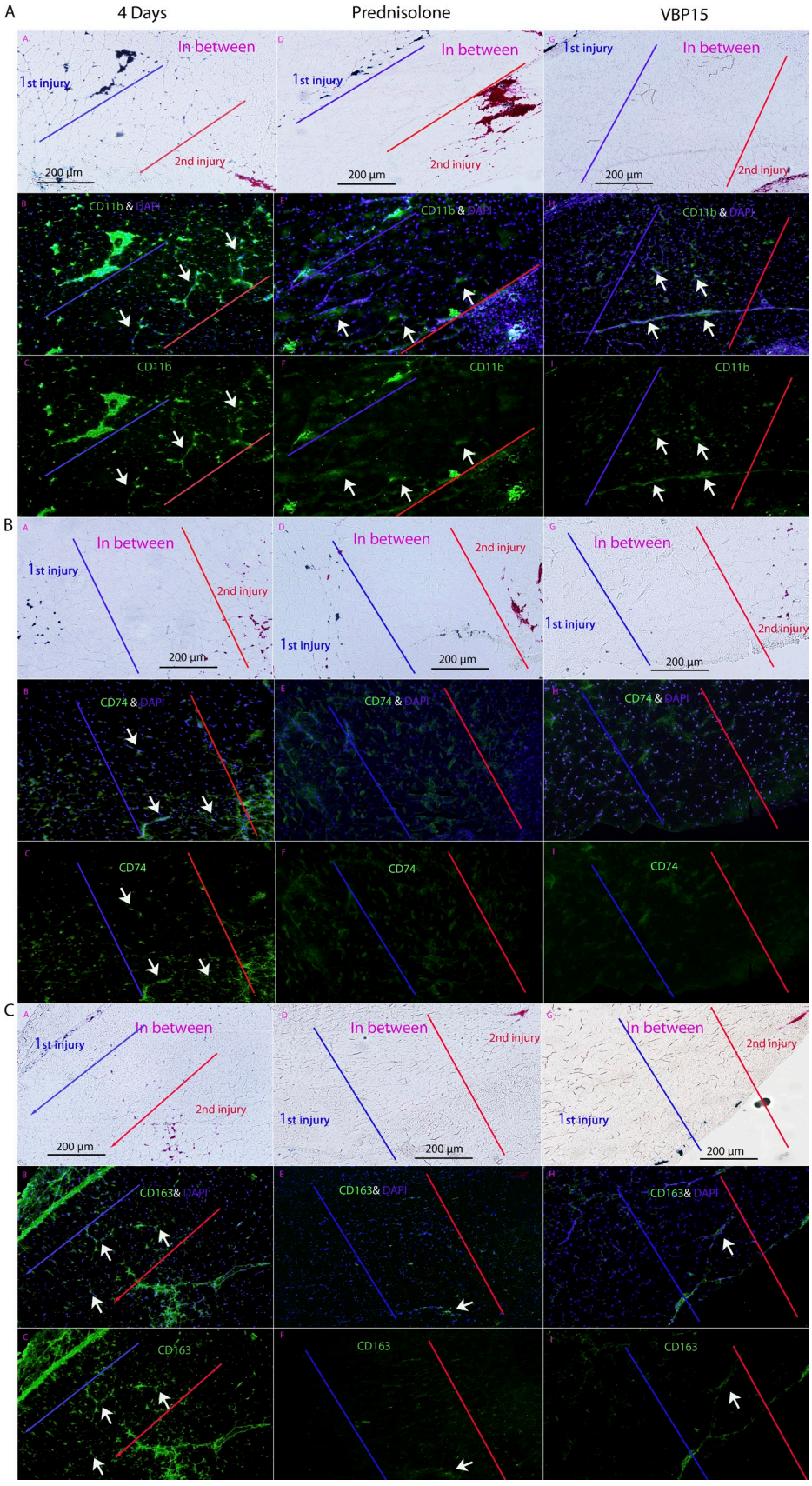

Figure S5. **Treatment of asynchronous remodeling mouse muscle with prednisone or VBP15 suppresses the proinflammatory proteins in between injuries spaced by 4 d.** (A–C) Shown is immunostaining of inflammatory proteins CD11b (A), CD74 (B), and CD163 (C) in muscles with repeated injuries spaced 4 d apart. Untreated (4 d), prednisolone-treated, and VBP15-treated mice were studied for expression of antigens at the injury sites marked by tattoo dyes. Expression of the three inflammatory markers was seen at high levels in between the injury sites in the nontreated muscle. This expression was suppressed by drug treatment (n = 3 muscle per group). Arrows indicate immunoreactive material in the microenvironment between two neighboring sites of regeneration.